

Pyrazolo-pyrimidines: A novel heterocyclic scaffold for potent and selective p38 α inhibitors

Jagabandhu Das,* Robert V. Moquin, Sidney Pitt, Rosemary Zhang, Ding Ren Shen, Kim W. McIntyre, Kathleen Gillooly, Arthur M. Doweiko, John S. Sack, Hongjian Zhang, Susan E. Kiefer, Kevin Kish, Murray McKinnon, Joel C. Barrish, John H. Dodd, Gary L. Schieven and Katerina Leftheris

Bristol-Myers Squibb Research and Development, PO Box 4000, Princeton, NJ 08543-4000, USA

Received 20 February 2008; revised 5 March 2008; accepted 6 March 2008

Available online 10 March 2008

Abstract—The synthesis and structure–activity relationships (SAR) of p38 α MAP kinase inhibitors based on a pyrazolo-pyrimidine scaffold are described. These studies led to the identification of compound **2x** as a potent and selective inhibitor of p38 α MAP kinase with excellent cellular potency toward the inhibition of TNF α production. Compound **2x** was highly efficacious in vivo in inhibiting TNF α production in an acute murine model of TNF α production. X-ray co-crystallography of a pyrazolo-pyrimidine analog **2b** bound to unphosphorylated p38 α is also disclosed.

© 2008 Elsevier Ltd. All rights reserved.

The mitogen activated protein kinase p38 is a serine/threonine kinase that exists in four isoform (α , β , γ , and δ). Expression of p38 isoforms varies among different cell types of the immune system and p38 α is believed to be the predominant isoform involved in inflammation.¹ Activation of p38 α leads to upregulation of pro-inflammatory cytokines such as TNF α and IL-1 β .² These cytokines are associated with the onset of inflammatory and autoimmune diseases such as rheumatoid arthritis (RA), Crohn's disease, psoriasis, and inflammatory bowel disease (IBD).³

Identification of potent and selective p38 α inhibitors as clinical candidates has therefore generated considerable interest in the pharmaceutical industry.⁴ We recently disclosed a series of 5-cyanopyrimidines **1** (Fig. 1) as potent inhibitors of the p38 α MAP kinase.^{4a} In an attempt to design novel chemotypes we envisioned that the incorporation of a ring constraint through cyclization of the 5-cyano and the 6-aminoalkyl functions of 5-cyanopyrimidines should lead to a pyrazolo-pyrimidine **2** (Fig. 1) which may serve as a novel scaffold for designing inhibitors.

In this letter, we describe the synthesis and structure–activity relationship (SAR) studies of the pyrazolo-pyrimidines that led to the identification of compound **2x** as a potent and selective p38 α inhibitor. Analog **2x** was also highly efficacious in vivo in an acute pharmacodynamic model of TNF α production in mice.

The synthesis of the pyrazolo-pyrimidine analogs follows some general routes as described in Schemes 1–3.

Preparation of analogs with a C-6 amino substituent (**2b–2j**) utilized readily available 4,6-dihydroxy-1-phenyl-pyrazolo-[3,4-*d*]pyrimidine **7**⁵ (Scheme 1) which upon treatment with phosphorous pentachloride and phosphorous oxychloride under reflux formed the corresponding 4,6-dichloro-adduct **8**. Reaction of **8** with aniline **9** in absolute ethanol in the presence of *N,N*-diisopropylethylamine formed exclusively the 4-anilino-adduct **10** which served as a common intermediate for the preparation of 6-amino substituted analogs. Accordingly, treatment of **10** with *N*-methyl-homopiperazine in isopropanol at elevated temperature formed analog **2d** in 60% yield.

The synthesis of 6-unsubstituted analogs (**2k–2r**) followed a similar route (Scheme 2). Accordingly, the reaction of amino-pyrazole **6** with formamide⁶ at 190 °C

Keywords: p38 α inhibitors; Pyrazolo-pyrimidines.

* Corresponding author. Tel.: +1 609 252 5068; fax: +1 609 252 6804; e-mail: jagabandhu.das@bms.com

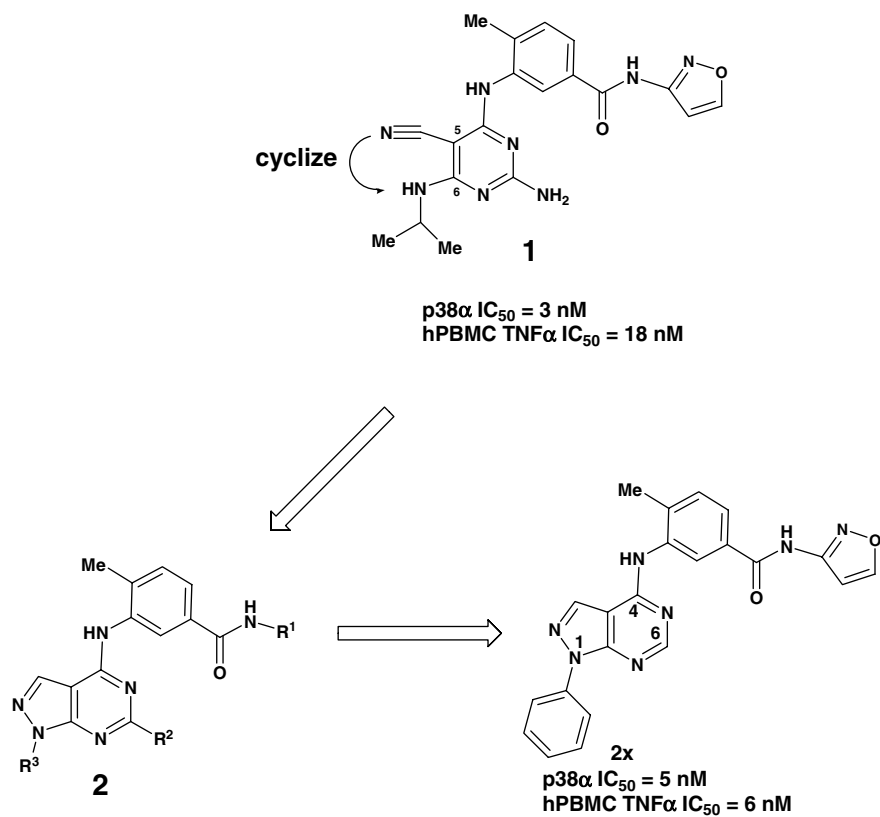
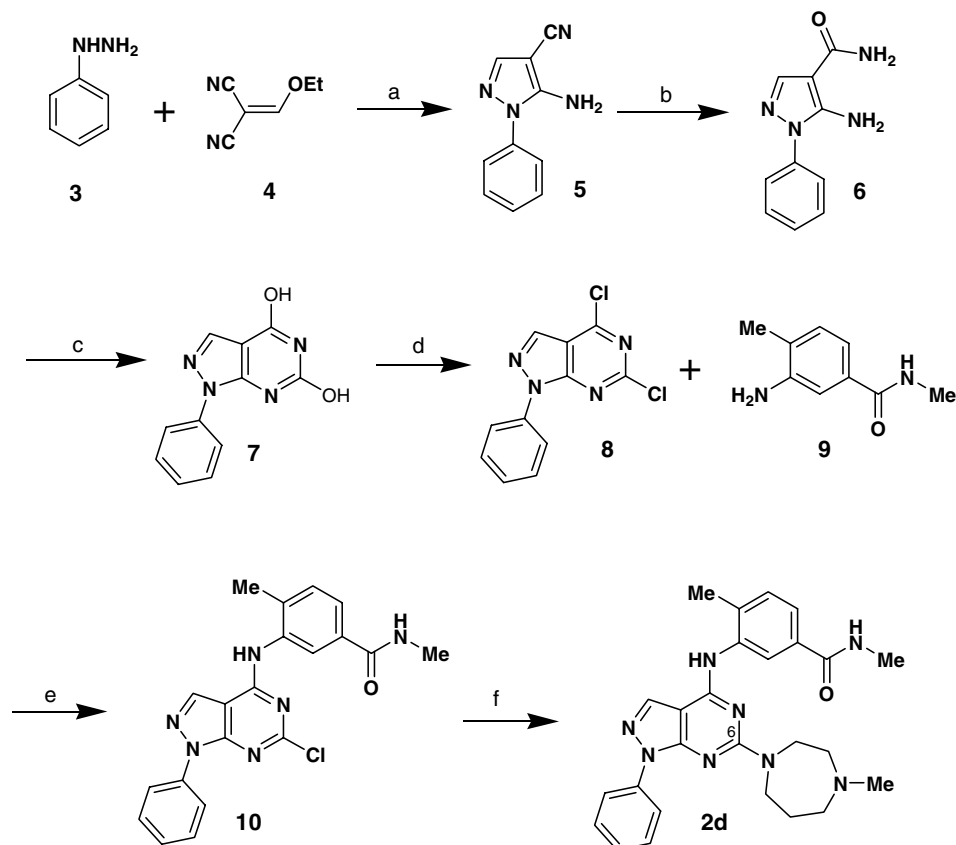
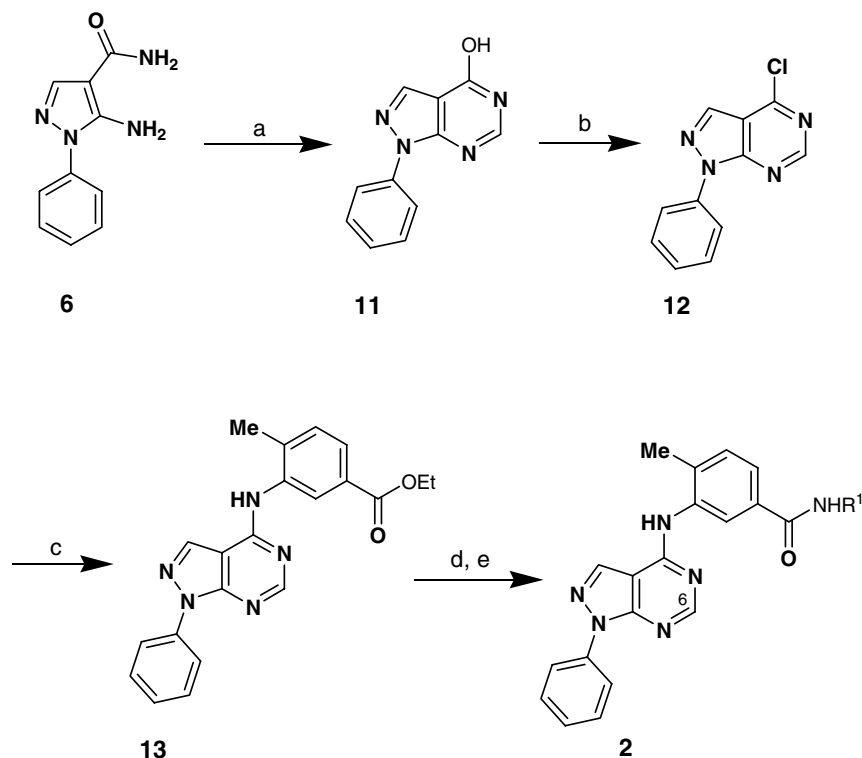


Figure 1. Activities of cyanopyrimidine **1** and pyrazolo-pyrimidine **2x**.



Scheme 1. Reagents and conditions: (a) EtOH, 60 °C, 1 h, 60%; (b) sulfuric acid, 0 °C to rt, 7 h, 90%; (c) urea, 200 °C, 3 h, 70%; (d) POCl₃, PCl₅, Δ , 3 h, 93%; (e) *i*-Pr₂NEt, EtOH, 60 °C, 4 h, 60%; (f) *N*-Me-homopiperazine, *i*-PrOH, 100 °C, 3 h, 60%.



Scheme 2. Reagents and conditions: (a) HCONH_2 , 190 °C, 3 h, 75%; (b) POCl_3 , 90 °C, 3 h, 85%; (c) ethyl-3-amino-4-methylbenzoate, EtOH, 140 °C, 1.5 h, 95%; (d) 1 N aq NaOH, THF–MeOH, rt, 16 h, 85%; (e) EDC, HOBT, THF–DMF, R_2NH_2 , $i\text{-Pr}_2\text{NEt}$, EtOH, 60 °C, 7 h, 55–100%.

formed 4-hydroxy-1-phenyl-pyrazolo-[3,4-*d*]pyrimidine **11**. Reaction of **11** with phosphorous oxychloride at elevated temperature afforded the 4-chloro derivative **12** which upon treatment with 2-methyl-5-carbomethoxy-aniline formed **13**. Saponification of ethyl ester **13** and subsequent treatment of the corresponding acid with an amine under standard coupling conditions afforded analogs **2**.

An alternate synthetic route was utilized for analogs with a 6-amino substituent and is illustrated with the synthesis of **2a** (Scheme 3).⁷ Base-catalyzed condensation of phenyl hydrazine **3** and 2-amino-4,6-dichloropyrimidine-5-carboxaldehyde **14** in refluxing THF formed 4-chloropyrimidine **15** which upon reaction with aniline **9** afforded analog **2a** in 40% overall yield in two steps.

The preliminary structure–activity optimization studies of pyrazolo[3,4-*d*]pyrimidines (**2**) are outlined in Tables 1–3. Compounds were evaluated for their ability to inhibit phosphorylation of substrate (myelin basic protein) by recombinant human p38 α .⁸ A peripheral blood mononuclear cell-based assay (hPBMC) was used to measure the ability of compounds to inhibit LPS-induced TNF α production in human primary cells.⁸

Table 1 summarizes some of the salient SAR findings for C-6 substitution in the pyrazolo-pyrimidine ring. The amino analog **2a** displayed excellent activity in the p38 α enzyme assay but was only moderately potent in the cellular assay. The corresponding methylamino analog **2b** is roughly 5-fold less potent. Both enzyme and cellular potencies of analog **2b** could be significantly improved by the attachment of a cyano ethyl side chain (**2c**) to the methylamino group. A similar boost in cellular potency was observed upon introduction of a polar pyrrolidinoethyl side chain (**2h**) in primary amine analog **2a**. Homopiperazine analog **2d** was identified as one of the most potent analogs in the amine series. A wide variety of substituents are tolerated at the C-6 position. Replacement of the amino group with hydrogen (**2e**),

Scheme 3. Reagents and conditions: (a) THF, Et_3N , Δ , 20 min, 78%; (b) EtOH–DMF, 146 °C, 0.5–1 h, 50%.

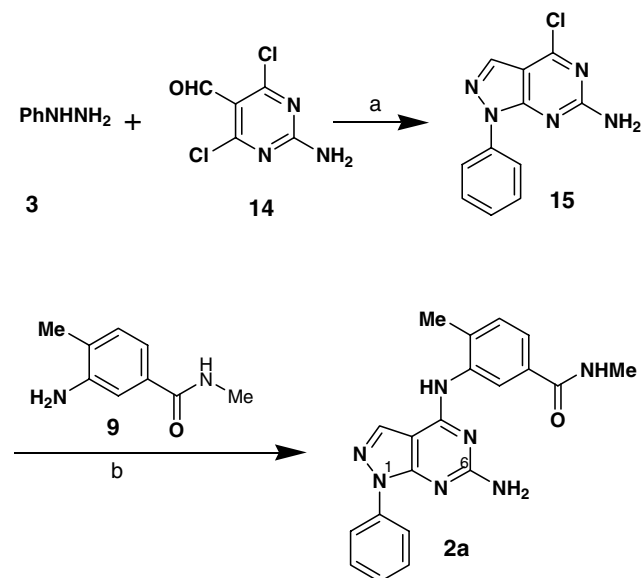
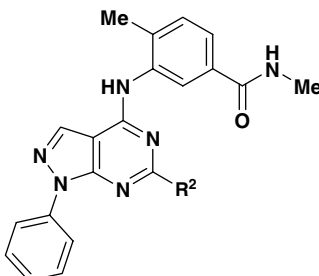
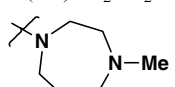
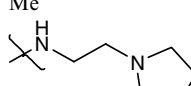
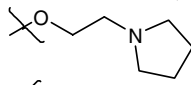
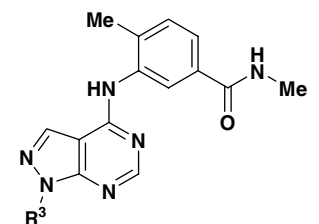


Table 1. SAR for C-6 substitution


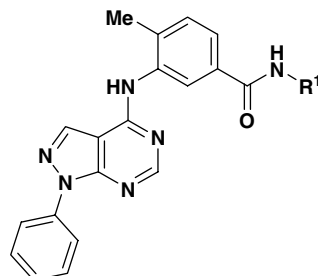
Compound	R ²	p38 α IC ₅₀ ^a (nM)	hPBMC TNF α IC ₅₀ ^b (nM)
2a	NH ₂	3	193
2b	NHMe	14	513
2c	N(Me)CH ₂ CH ₂ CN	5	43
2d		8	16
2e	H	10	67
2f	OMe	11	>2000
2g	Me	18	>2000
2h		4	36
2i		6	27
2j		12	290

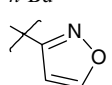
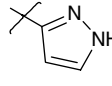
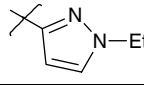
^a n = 4, variation in individual values, <20%.^b n = 3, variation in individual values, <25%.

alkoxy (**2f**), or alkyl (**2g**) retained most of the p38 α enzyme activity. However, analogs **2f** and **2g** were found to be significantly less potent in the cell-based assay. Fi-

Table 2. SAR for N-1 substitution


Compound	R ³	p38 α IC ₅₀ ^a (nM)	hPBMC TNF α IC ₅₀ ^b (nM)
2k	Me	253	—
2l	<i>tert</i> -Butyl	13	>250
2e	Ph	10	67
2m	CH ₂ Ph	13	292
2n	2-Pyridyl	67	801
2o	2-F-phenyl	9	50
2p	2,6-Di-Cl-phenyl	6	>250
2q	2,4,6-Tri-Me-phenyl	24	50
2r	4-F-phenyl	9	220

^a n = 4, variation in individual values, <20%.^b n = 3, variation in individual values, <25%.**Table 3.** SAR for side chain carboxamide modification


Compound	R ¹	p38 α IC ₅₀ ^a (nM)	hPBMC TNF α IC ₅₀ ^b (nM)
2s	H	7	635
2t	OMe	4	19
2e	Me	10	67
2u	Bn	184	—
2v	3-Pyridyl	240	1480
2w	<i>n</i> -Bu	21	>2000
2x		5	6
2y		3	64
2z		8	<8

^a n = 4, variation in individual values, <20%.^b n = 3, variation in individual values, <25%.

nally, the replacement of the methoxy group with a pyrrolidino-ethoxy substituent (**2i**) resulted in significant improvement in both biochemical and cellular potencies and is consistent with our earlier observation with C-6 amino substituted analogs (**2b** and **2h**). Because of its excellent potency, the C-6 unsubstituted analog **2e** was selected for further SAR optimization.

In order to further improve the cellular potency in the methyl carboxamide series, we turned our attention to the effect of substitution at the N-1 position of the pyrazolo-pyrimidine ring. Some salient SAR findings on analog **2e** are reported in Table 2. Replacement of the phenyl group with alkyl groups showed mixed results. The N-1 Me analog **2k** was about 25-fold less potent than the phenyl derivative **2e**, while the *tert*-butyl analog **2l** retained the potency in vitro. However, analog **2l** is significantly less potent than compound **2e** in the cellular assay. Similarly the phenyl ring could be replaced with a benzyl (**2m**) with some attenuation in cellular potency. However, the replacement of the phenyl ring with a pyridyl ring (**2n**) resulted in several fold drop in both enzyme and cellular activities. In contrast, substitution(s) on the phenyl ring (**2o–2r**) was tolerated. The 2-F-phenyl analog **2o**, and the 2,4,6-trimethylphenyl analog **2q** were equipotent to **2e** in both the biochemical and cellular assays.

A more pronounced improvement in potency was observed during the SAR investigation of the carboxamide

modification in the pendant aniline ring (Table 3). It should be noted that the relative positions of the methyl, carboxamide, and the amino group in the pendant aniline ring were critical for the p38 α enzyme activity. Removal or transposition of the methyl and the carboxamide groups resulted in several orders of magnitude loss in biochemical potency (data not shown). The primary carboxamide analog **2s** was significantly less potent in the cellular assay despite retaining the biochemical activity relative to the methyl amide **2e**. In contrast a substantial increase in both biochemical and cellular potencies was observed upon the substitution of the methyl amide with a methoxy amide (**2t**). The replacement of the methyl amide with either a benzyl (**2u**), pyridyl (**2v**) or long chain alkyl amide (**2w**) was detrimental for enzyme activity. A significant improvement in biochemical potency and a more dramatic increase in cellular potency were observed upon replacement of the methyl amide with five-membered heterocyclic amides, most notably iso-oxazole (**2x**), and N-Et pyrazole (**2z**). Analogs **2x** and **2z** were thus identified as two of the most potent p38 α inhibitors in this series.

Based on its p38 α inhibitory potency, acceptable liability profile, and in vitro metabolic stability, analog **2x** was selected for further evaluation. Compound **2x** was characterized as a highly potent inhibitor of human p38 α enzyme with a K_i value of 0.2 nM, excellent metabolic stability with microsomal metabolic rates of 0.000 and 0.005 nmol/min/mg protein, respectively, in humans and rats. Analog **2x** also displayed a clean profile against CYP 450 inhibition with IC₅₀ values of >40 μ M for 1A2, 2C9, 2C19, 2D6, and 3A4 isozymes. The kinase selectivity profile of **2x** was determined against several receptor and non-receptor tyrosine kinases, as well as serine/threonine kinases (Table 4). Compound **2x** was shown to be at least 1000-fold selective over 20 different kinases. Furthermore, a close analog in this series, compound **2b** was found to be a selective p38 α inhibitor (IC₅₀ = 14 nM) over p38 γ and δ (IC₅₀s > 30 μ M). No selectivity was observed in the inhibition of p38 β isoform (IC₅₀ = 12 nM).

The pharmacokinetic profile of compound **2x** was determined in mice. Upon oral dosing at 10 mg/kg, analog **2x** was determined to be highly bioavailable ($F\%$ 60) with a low clearance rate (0.3 L/kg/h), high volume of distribution (1.3 L/kg), and acceptable terminal half-life ($t_{1/2}$ =

4.1 h). The in vivo efficacy of **2x** was demonstrated in an acute pharmacodynamic model of LPS-induced TNF α production in mice. Mice were dosed orally with **2x** at 5 mg/kg, 5 h prior to LPS administration and the plasma TNF α level was measured 90 min after the LPS challenge. In this model, compound **2x** inhibited circulating TNF α level by >70%.⁸

To understand the binding mode of this novel pyrazolo-pyrimidine class of p38 α inhibitors, compound **2b** was co-crystallized with purified, unphosphorylated p38 α MAP kinase and the X-ray structure of the complex was determined.^{8,9} The key binding interactions between compound **2b** and the p38 α enzyme are illustrated in Figure 2.

The X-ray structure of **2b** complexed with p38 α reveals a combination of H-bonding and hydrophobic interactions. Consistent with our previous findings with related p38 α inhibitors, the pendant carboxamido-aniline ring occupies an angular hydrophobic pocket and makes key hydrogen-bond interactions. More specifically, the aniline NH is in H-bonding distance with Thr106 (2.01 Å) and the carboxamido NH is engaged in an H-bond interaction with Glu71 (2.07 Å). The hinge region residue, Met109 NH forms an H-bond with 2' position nitrogen of the pyrazole. This 2' pyrazole nitrogen corresponds to the nitrile N of the cyanopyrimidine **1**. The phenyl ring attached to the pyrazolo-pyrimidine ring is skewed out of plane. This orientation may explain some of the SAR observed regarding substitution at the *ortho*-position of the pendant phenyl ring.

In conclusion, we have identified a series of exquisitely potent and selective p38 α inhibitors using a novel pyrazolo-pyrimidine scaffold. SAR optimization on different fragments of this ring system led to the identification of analog **2x** as one of the most potent p38 α inhibitor in this series with single digit nanomolar potency for the inhibition of TNF α release in human peripheral blood mononuclear cells (PBMCs). Oral efficacy was

Table 4. Kinase selectivity profile of **2x**

Kinase	IC ₅₀ (μ M)	Kinase	IC ₅₀ (μ M)
p38 α	0.005	Jak3	>50
KDR	>10	Lck	>50
Akt	>50	FGFR1	>50
CaMKII	>50	SYK	>50
Cdk2	>10	MK2	>30
Itk	>50	ERK	>50
Raf	>30	PKA	46
FGF	>50	PKC α	188
GSK3	>5	PKC δ	40
HER1	>50	PKC τ	>40
IGF-1R	>25	PKC ζ	>40

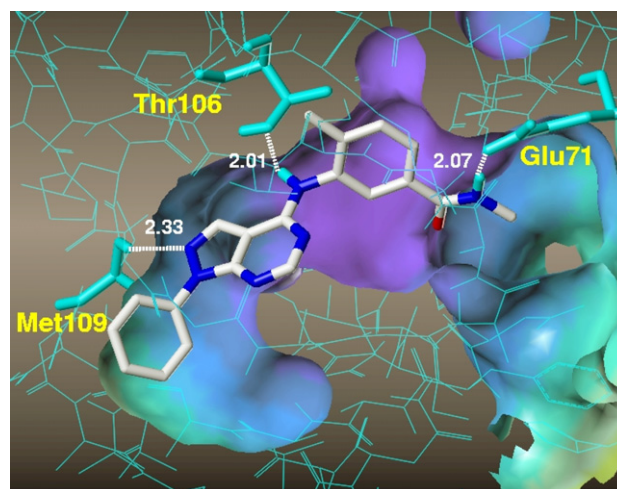


Figure 2. Binding interactions between **2b** and unphosphorylated p38 α based on X-ray crystallographic analysis. Hydrogen-bond distances are given in angstroms with key protein residues labeled.

also demonstrated with this analog in an acute murine model of TNF α inhibition. In addition, the molecular basis for p38 α inhibition of this class of inhibitor was established via X-ray crystal structure determination of an enzyme–inhibitor complex.

References and notes

- (a) Hale, K. K.; Trollinger, D.; Rihanek, M.; Manthey, C. L. *J. Immunol.* **1999**, *162*, 4246; (b) Allen, M.; Svensson, L.; Roach, M.; Hambor, J.; McNeish, J.; Gabel, C. A. *J. Exp. Med.* **2000**, *191*, 859; (c) Fearn, C.; Kline, L.; Gram, H.; Di Padova, F.; Zurini, M.; Han, J.; Ulevitch, R. J. *J. Leukocyte Biol.* **2000**, *67*, 705.
- (a) Schieven, G. L. *Curr. Top. Med. Chem.* **2005**, *5*, 921; (b) Saklatvala, J. *Curr. Opin. Pharm.* **2004**, *4*, 372; (c) Kumar, S.; Boehm, J.; Lee, J. C. *Nat. Rev. Drug Discov.* **2003**, *2*, 717; (d) Adams, J. L.; Badge, A. M.; Kumar, S.; Lee, J. C. *Prog. Med. Chem.* **2001**, *38*, 1; (e) Lee, J. C.; Laydon, J. T.; McDonnell, P. C.; Gallagher, T. F.; Kumar, S.; Green, D.; McNulty, D.; Blumenthal, M. J.; Heys, J. R. *Nature* **1994**, *372*, 739.
- (a) Wagner, G.; Laufer, S. *Med. Res. Rev.* **2006**, *26*, 1; (b) Westra, J.; Limburg, P. C. *Mini-Rev. Med. Chem.* **2006**, *6*, 867.
- (a) Liu, C.; Wroblewski, S. T.; Lin, J.; Gillooly, K. M.; McIntyre, K.; Pitt, S.; Shen, D. R.; Shuster, D. J.; Zhang, H.; Doweyko, A. M.; Sack, J. S.; Barrish, J. C.; Dodd, J. H.; Schieven, G. L.; Leftheris, K. *J. Med. Chem.* **2005**, *48*, 6261; (b) Hynes, J.; Leftheris, K. *Curr. Top. Med. Chem.* **2005**, *5*, 967; (c) Miwatashi, S.; Arikawa, Y.; Kotani, E.; Miyamoto, M.; Naruo, K.; Kimura, H.; Tanaka, T.; Asahi, S.; Ohkawa, S. *J. Med. Chem.* **2005**, *48*, 5966; (d) Goldstein, D. M.; Gabriel, T. *Curr. Top. Med. Chem.* **2005**, *5*, 1017; (e) Diller, D. J.; Lin, T. H.; Metzger, A. *Curr. Top. Med. Chem.* **2005**, *5*, 953; (f) Dominguez, C.; Powers, D. A.; Tamayo, N. *Curr. Opin. Drug Discov. Devel.* **2005**, *8*, 421.
- Cheng, C. C.; Robins, R. K. *J. Org. Chem.* **1958**, *23*, 852.
- Cheng, C. C.; Robins, R. K. *J. Org. Chem.* **1956**, *21*, 1240.
- Seela, F.; Steker, H. *Helv. Chim. Acta* **1986**, *69*, 1602.
- For a description of the biological assays, and X-ray crystal structure determination protocol, see Hynes, J., Jr.; Dyckman, A. D.; Lin, S.; Wroblewski, S. T.; Wu, H.; Gillooly, K. M.; Lonial, H.; Loo, D.; McIntyre, K. W.; Pitt, S.; Shen, D. R.; Shuster, D. J.; Zhang, X.; Behnia, K.; Marathe, P. H.; Doweyko, A.; Barrish, J.; Dodd, J.; Schieven, G.; Leftheris, K. *J. Med. Chem.* **2008**, *51*, 4.
- The X-ray coordinates have been deposited with RCSB Protein Data Bank Database (RCSB ID Code rcsb046732 and PDB ID Code 3CG2).